

Development of a Five-Fingered Biomimetic Soft Robotic Hand by 3D Printing the Skin and Skeleton as One Unit

Kazuhiro Miyama¹, Kento Kawaharazuka¹, Kei Okada¹, and Masayuki Inaba¹

Abstract—Robot hands that imitate the shape of the human body have been actively studied, and various materials and mechanisms have been proposed to imitate the human body. Although the use of soft materials is advantageous in that it can imitate the characteristics of the human body’s epidermis, it increases the number of parts and makes assembly difficult in order to perform complex movements. In this study, we propose a skin-skeleton integrated robot hand that has 15 degrees of freedom and consists of four parts. The developed robotic hand is mostly composed of a single flexible part produced by a 3D printer, and while it can be easily assembled, it can perform adduction, flexion, and opposition of the thumb, as well as flexion of four fingers.

I. INTRODUCTION

Robots are being used to automate tasks previously performed by humans, with robot hands playing a particularly important role. In a social implementation, changing hands according to the task is problematic in terms of implementation cost. However, a robot hand that can perform many tasks with a single hand has advantages such as greatly reducing the cost of introduction and contributing greatly to the realization of an automated society. Most tools in society are made to fit human hands, so the human mimetic robot hand can be implemented in society without the use of special tools.

Among the human mimetic robot hands, the soft robot hand is particularly effective. Because the organs of the human body, such as the epidermis and tendons, are composed of flexible materials similar to those of the soft robotic hand, the human body can be imitated more faithfully than with a rigid robotic hand. According to Shimago et al.’s study [1], the use of soft materials in robotic hands has been shown to have three useful properties: a) impact force attenuation, b) conformability, and c) repetitive strain. These human mimetic robotic hands have been studied for applications such as the reproduction of human tasks [2] as well as for the study of human anatomy [3] [4].

Soft-material human mimetic robot hands have advantages in terms of hardware and ease of assembly. In general, rigid robot hands have a large number of parts, and human body-mimetic robot hands in particular are highly complex because they require multiple degrees of freedom. For example, the ShadowHand [5] has 40 actuators and 20 DoF, making it difficult to maintain. On the other hand, the soft robot hand does not need to attach axes and bearings by deforming each

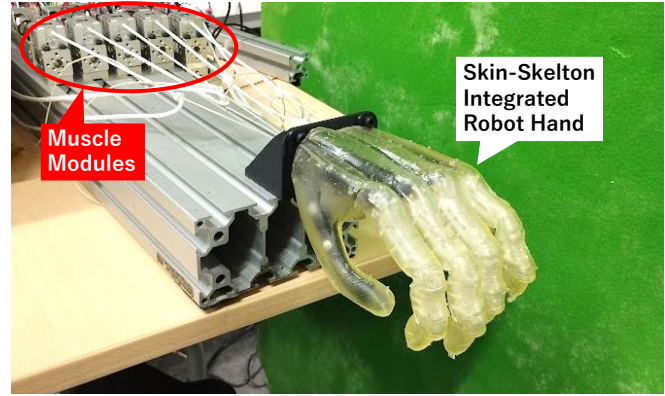


Fig. 1. Overview of skin-skeleton integrated robot hand

axis with flexibility, and can even use bellows [6] etc., thus reducing the number of parts.

However, there is a problem in that the number of joints and controllability decreases due to the simple design with fewer parts. Methods to realize other degrees of freedom with a soft robot hand include covering the exterior of a rigid robot hand with soft materials [7] [8] or designing a chamber inside and having it driven by pneumatic pressure [9] [10]. But the former method does not reduce the number of parts, and the latter method involves a complex process of layering several layers of silicon to prevent air leakage.

In order to solve the problem mentioned above while taking advantage of the soft robot hand, the objective of this study is to develop a soft robot hand that combines the complexity of the model with the simplicity of assembly.

We propose a skin-skeleton integrated robot hand (Fig. 1) that is driven by wires and molded by an optical 3D printer using the same material for the skin and the skeleton to achieve this objective.

Robot hands using 3D printers have been studied extensively in the field of soft robotics in recent years. There are methods such as a robot hand that is driven by air pressure by creating a cavity [11] or a hand that is shaped as a single piece [12], but from a practical standpoint, the low rigidity, the small number of grasping postures that can be realized, and the complexity of the air-driven hand are issues to be solved. There is research on the use of FDM 3D printers to make the skin and skeleton of the hand itself as a single piece [13], but the FDM method cannot create a hollow space in the part, which weakens the advantage of Shimago’s c) repetitive strain dissipation. The skin-skeleton integrated robot hand is a light fabrication method, which has a skeleton shape and hollow space inside, and is wire-driven, so we thought that

¹ The authors are with the Department of Mechano-Informatics, Graduate School of Information Science and Technology, The University of Tokyo, 7-3-1 Hongo, Bunkyo-ku, Tokyo, 113-8656, Japan. [miyama, kawaharazuka, okada, inaba]@jsk.t.u-tokyo.ac.jp

both rigidity and structural simplicity could be achieved.

This robot hand has the following three features. First, the majority of the hand is composed of a single part, the skin-skeleton integral part, and the entire robot hand is composed of four parts. This simplifies assembly and fabrication, and all parts can be completed simply by sending the model data to a 3D printer. The assembly method is also simple: wires are threaded through the skeleton-skin parts and combined with the metacarpal and thumb parts, and the robot can be completed in less than an hour.

Second, the item grasping performance is high. Since the skin-skeleton integrated robot hand has the characteristics of a soft robot hand, it can manipulate a variety of items by grasping utilizing friction and deformation. In addition, since it is a multi-degree-of-freedom under-driven robot hand with five fingers driven by wires, various postures can be realized, which also contributes to improved grasping performance.

The third is shock resistance. Because it has soft joints, it can return to its initial posture immediately, although it is greatly deformed when an impact is applied. Therefore, it has high adaptability to the environment and has the potential to be used for cooperation and interaction with humans.

In Section II, we describe the outline and overall design of the skin-skeleton integrated robot hand. In Section III, we explain the design of the joints and the palm of the skin-skeleton integrated parts that will be output by the stereolithography 3D printer and verify the effect by experiments. In Section IV, the remaining components of the skin-skeleton integrated robot hand, the metacarpal and thumb, are described and their assembly is explained. In Section V, several experiments including grasping experiments using the skin-skeleton integrated robotic hand are conducted to verify its effectiveness as a robotic hand. In Section VI, we conclude the performance of the skin-skeleton integrated robot hand based on the experimental results.

II. OVERVIEW OF THE SKIN SKELETON-INTEGRATED ROBOT HAND

The overall view of the skin-skeleton integrated robot hand is shown in Fig. 1. This robot hand has a five-finger skeletal structure that mimics the human hand and is driven by seven wires (hereinafter referred to as tendons). The index, middle, ring, and little finger, excluding the thumb, have one tendon for each finger, and the flexion motion is performed by pulling the tendon. The extension motion of these fingers is performed by the elasticity of the joints. The thumb is driven by three wires, and the placement of the wires and other details are described in detail in Section II-A.

The robot hand is composed of a skin-skeleton integrated part, a metacarpal part, and a thumb part. The skin-skeleton integrated part is made of a Shore hardness 50A soft material (Elastic 50A, RS-FL-ENG-E50A) and is fabricated using a light-molded 3D printer (SLA, Stereo Lithography Apparatus) Form3. On the other hand, the metacarpal and thumb are made of ABS filament. The overall dimensions of the robot hand are based on the AIRC hand size data [14], and the diameter and joint lengths are set to be similar to those of an adult male.

A. Comparison with the human hand

We will compare this robot hand with a human hand (Fig. 2). First, we discuss the four fingers, excluding the thumb. They have three joints: the DIP joint, the PIP joint, and the MP joint, which are made up of four bones: the distal phalanx, middle phalanx, proximal phalanx, and metacarpal bones. The flexor digitorum profundus, flexor digitorum teres, and interosseous muscles are allocated to each of these joints, and the DIP, PIP, and MP joints are driven by the flexor digitorum profundus, and the PIP and MP joints are driven by the flexor digitorum superficialis. This robot hand reproduces the flexor digitorum profundus that drives the three joints simultaneously and realizes flexion movements by placing one tendon on each finger. Although human fingers also have dorsal interosseous muscles for adduction and abduction, these muscles are not used for grasping and tool manipulation, so they were not employed in this study.

The thumb in the human body is similar to the other four fingers in that it has an IP joint and MP joint with the distal phalanx, proximal phalanx, and metacarpal bones, but it is unique in that the CM joint, the joint where the metacarpal bone is connected to the wrist side, has two degrees of freedom. In other words, the complexity of the thumb is established by the flexion-extension of the MP joint as well as the adduction-abduction and opposition-resumption of the CM joint. The flexor pollicis muscle and extensor pollicis muscle are responsible for flexion and extension, the adductor pollicis muscles and abductor pollicis muscles are responsible for adduction and abduction, and the opponens pollicis muscle and retractor pollicis longus muscles are responsible for opposition and return. In this robot hand, the flexor pollicis brevis muscle, adductor pollicis muscles, and opponens pollicis muscle are used to drive the thumb. This robot hand has the same degrees of freedom as the human body and is driven by three tendons. Details on the drive of the thumb will be described in detail in Section IV.

The functions of the palms are also compared. The palm can be broadly divided into four parts by the MP joints, the thenar muscles, and the hypothenar muscles. By moving the MP joints of each finger, the shape of the palm can be changed to assume various postures, such as holding or pinching an object. The details will be described in Section III-D, but for this robot hand, we also designed the palm for flexion of the MP joints and movement of the CM joints of the thumb.

The human body is said to have 20 DoFs, and this robot hand has 15 DoFs, 3 DoFs for each of 5 fingers.

III. DESIGN OF SKIN-SKELETON INTEGRATED PART

This chapter describes the skin-skeleton-integrated part, which is the largest component of the robot hand (Fig. 3). This part consists of a model that mimics the epidermis of the human body, with the distal phalanx, middle phalanx, and proximal phalanx of the second to fifth fingers. The epidermis and the skeleton are connected by a layer of fat called the fat layer. The fat layer is a plate-like model about

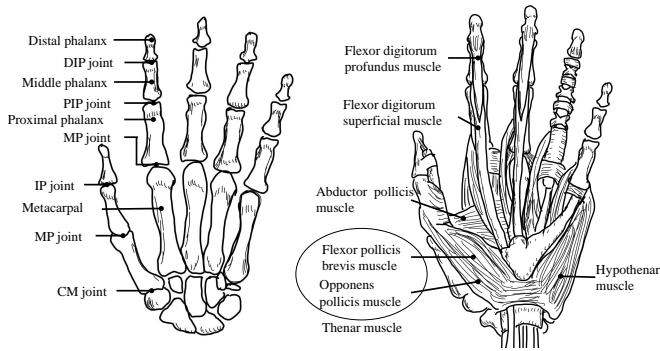


Fig. 2. Structure of the human hand and names of its parts

1[mm] thick that extends from the skeleton to the epidermis at equal intervals to anchor the skeletal parts.

As mentioned above, this part is produced by SLA 3D printer, which is difficult for commonly used Fused deposition modeling (FDM) 3D printers. The FDM printer can print filaments such as TPU with similar hardness to the resin used in this study, but it is difficult to model as designed because many supports are required for the framework inside the skin, and the strength in the direction parallel to the stacking direction is weak. However, the use of SLA printers makes it possible to avoid using supports inside the skeleton and to ensure strength regardless of the stacking direction.

The thickness of the skin is a trade-off between break resistance and flexibility. If it is too thin, it will break due to impact or tension, while if it is too thick, it will break due to folding during flexion, in addition to not providing flexibility. As a result of testing several thicknesses, it is confirmed that the thickness of 2[mm] for most parts of the robot hand and 0.5[mm] for parts where flexibility is required, such as joints, is the method that causes the fewest ruptures, and this method is adopted in this study as well. The following four points are considered important in the design of this robot hand.

- 1) Structure of joints
- 2) Design of skeletal and tendon
- 3) Initial posture
- 4) Palm flexibility

The next subsections will discuss these in more detail.

A. Structure of the Joint of Skin-Skeleton Integrated Parts

First, the joint structures of the four fingers, excluding the thumb, are described. The material used in the fabrication of this robot hand was a flexible material with a Shore hardness of 50A and an elongation at break of 160%. However, since the breaking tensor was as low as 3.2 MPa, it was confirmed that the material would break under pressure, such as when folded or pulled. Therefore, holes are designed on the palm side of the four finger joints (the same at the PIP, DIP, and MP joints), and a structure with exaggerated human wrinkles on the dorsal side (only at the PIP and DIP joints). The holes on the palm side serve to prevent folding and breaking during flexion, while the wrinkles on the dorsal skin are designed to prevent tearing through extension.

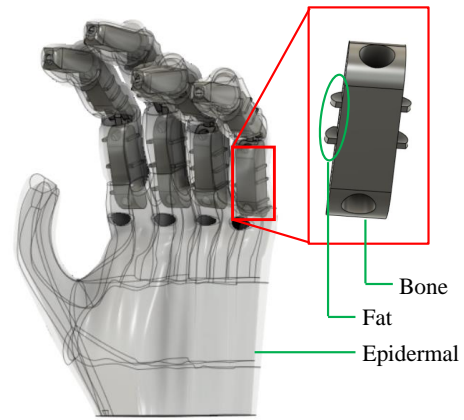


Fig. 3. Overview of skin-skeleton integrated parts

In addition to this, the skin was designed to be about 0.5[mm] thick around the joints, whereas the thickness of the surrounding skin is about 2[mm], to encourage more bending. In order to promote deformation due to pressure, we also design the palm side of the hand to create a layer of air. This resulted in a system that increases the contact area upon contact with an object on the human body, with the epidermal part deforming until it hits the skeletal part.

Experiments were conducted to verify the effect of the additional design of dorsal-side wrinkles and palm-side holes in the finger joints: 1) a model of the proposed method with holes on the palm side and wrinkles on the dorsal side, 2) a model with holes on the palm side and a flat dorsal side, 3) a model without holes on the palm side and wrinkles on the dorsal side, 4) a model without holes on the palm side and wrinkles on the dorsal side. The models of each of the four types of fingers were created (Fig. 4) and the tension in flexion was measured with the attached load cell while fixed to the muscle module [15]. The resulting graphs and maximum tension are shown in Fig. 5 and Table I.

The blue line in Fig. 5 is the value of the maximum tension of the proposed method. From these results, there was no model that required less tension for bending than the proposed method. 2) and 3) Both methods were found to require less tension for bending when there was a slight wrinkle, although there was no significant difference. However, it was found that the absence of either element required 166% more tension to perform the flexion action than the presence of either element. These results confirm that the dorsal-side wrinkle and the palm-side hole contribute to the reduction of tension for the flexion movement.

TABLE I
CHARACTERISTICS OF THE FINGERS USED IN THE EXPERIMENT AND THE MAXIMUM TENSION

	Hole on palm side	No Hole
Wrinkle on dorsal side	52.7[N]	63.9[N]
No Wrinkle	57.6[N]	87.8[N]

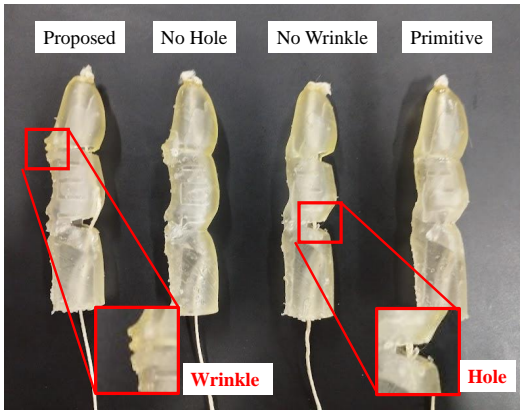


Fig. 4. Finger models used in tension tests

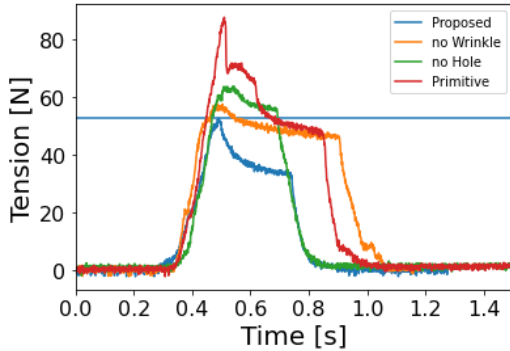


Fig. 5. Resulting graph of tension due to flexion of each finger model.(The blue line is the maximum tension of the proposed method)

B. Design of the Skelton and Tendon

In this section, the skeletal and tendon structures are described. The size of the skeleton, as well as the entire finger, is based on the AIRC hand dimension data [14], and based on the data, the design was made so that the distal:middle:basal segments are approximately 2:3:5. A cross-sectional view of the index finger is shown in Fig. 6. The joint is designed as a hinge at the center of rotation, which prevents the finger from shifting in the adduction-abduction direction.

The tendons for drive are placed inside the skeleton. Although tendons in the human body exist on the outside of the skeleton, the problem of high pressure applied to the epidermis by the stretched tendons arose when reproduced in this robot hand. In the human body, a thin membrane-like organ called the tendon sheath covers the tendon and drives the tendon while it remains closely attached to the finger bone. Although attempts to reproduce this in the robot hand would place high pressure on the thin tendon sheath, two problems arise when the tendon is placed without the tendon sheath. One is that the moment arm becomes too large, resulting in a small joint flexion angle, and the other is that the epidermis is subjected to high pressure from the tendon. Since experiments using tendons placed on the outside of the skeleton confirmed rupture of the epidermis, we decided to use a method in which the tendons are placed inside the skeleton.

The hole inside the skeleton as a guide for the tendon is curved to secure the moment arm to drive the tendon. Here, using the DIP joint of the Fig. 6 as an example, the center of rotation is considered as the red point in the figure. When the wire guide is placed at the centerline of the skeleton, the moment arm was 5.6 [mm]. In contrast, by placing the wire at a distance of a from the end point of the skeleton and at an angle of θ to the center line, the moment arm of $a \tan \theta$ can be increased. The value of a at the DIP joint of the index finger is 3 [mm] and θ is 30° , indicating an increase in moment arm of 25%. When the wire guide inside the skeleton is aligned with the centerline, it did not flex properly due to the tendon path and moment arm problem, but by properly designing the wire guide inside the skeleton, flexion was possible and the required tension was greatly reduced. The moment arm of the human joint protected by the tendon sheath is 7.5[mm] [16], which is similar to the 7.0[mm] of this robot hand.

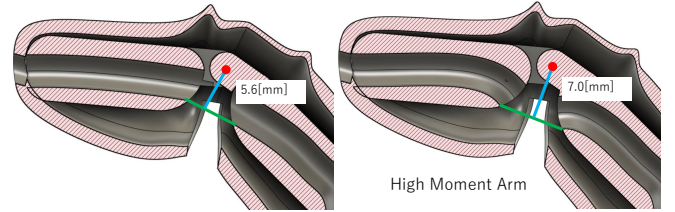


Fig. 6. Cross section of the index finger and moment arm of the PIP joint

C. Initial Posture of the Robot Hand

The initial posture of this robot hand is slightly flexed, which is designed to mean the balanced position of the muscles on the extension and flexion sides. The human hand has muscles and tendons on the flexion side and the extension side, and in the natural state when both muscles are relaxed, the hand is in a slightly flexed position. Since this robot hand has an actuator only on the flexion side while the extension side is restored by elasticity, we thought it would be unnatural to design it in the extended state.

Therefore, the initial angles of the finger joints, which were confirmed in experiments using cadavers [17], are used as a reference, and the initial postures are 35° for the MP joint, 40° for the PIP joint, and 15° for the DIP joint from the fully extended state. This reduced the angular change required for flexion and decreased the tension required for grasping.

D. Design of Palm

As described in Section II-A, the palm structure is divided into four parts by the MP joints, the thenar muscles, and the hypothenar muscles. Comparative images of the objects used in the design and the completed epidermal-skeletal integrated model are shown in Fig. 7. It is assumed that object B is fixed and object D is the movement of the thumb. The red edges are joined to each object, and the thumb is designed to achieve opposing motion by adjusting the length of each edge while moving object D.

The part where the objects cut each other is made to bend easily as designed by varying the thickness of the model. In particular, since the area where the thenar muscles exist in the human body (object D) is subject to large deformations, we made it easier to fold it during the opposing motion by designing it to be bulged.

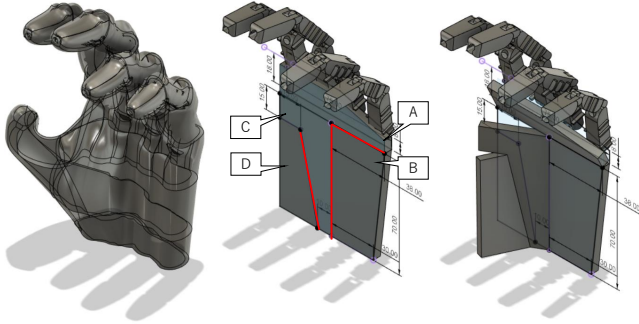


Fig. 7. Comparison of the objects used to design palm of the epidermis

IV. DESIGN OF OTHER PARTS, AND HOW TO ASSEMBLE THE ROBOT HAND

A. Design of thumb and metacarpals parts

In this section, the remaining components of the skin-skeleton integrated robot hand, the thumb and metacarpal parts, are described by comparing them with the human skeleton and tendon arrangement. The human thumb has three bones: the distal phalanx, proximal phalanx, and metacarpal bones, while the robot hand consists of two parts: a component joining the distal phalanx and proximal phalanx and a metacarpal bone. Although the movement of the distal phalanx contributes to the grasping and hooking of small objects, it does not contribute to the realization of various grasping postures or the grasping of large objects, so it was omitted. The CM joint with two degrees of freedom, which is a characteristic of the thumb, is a spherical joint together with the metacarpal parts.

The wire path of the thumb is shown in Fig. 8. As mentioned in Section II-A, of the seven muscles used to drive the thumb, only the flexor pollicis brevis muscle, abductor pollicis muscles, and opponens pollicis muscle are reproduced. The first is the flexor pollicis brevis muscle, which is the muscle used to flex the MP joint and is connected from the thumb basal bone to the flexor digitorum branch located in the wrist area. The second is the adductor pollicis brevis muscle, which contributes to the adduction movement that fans out from the proximal phalanx to the metacarpals of the metacarpals of the thumb. The second is the adductor pollicis brevis muscle, which contributes to the adduction movement that fans out from the proximal phalanx to the metacarpals of the metacarpals of the metacarpals of the thumb. The last, the opponens pollicis muscle, connects the metacarpal to the palmar carpal ligament, with the wires placed along a similar pathway.

The metacarpal bone is responsible for bringing together the tendons from the four fingers of the epidermal-skeletal

integrated part and passing them to the wrist side. It is also made of ABS filament, which does not deform when tension is applied and improves the rigidity of the entire hand.

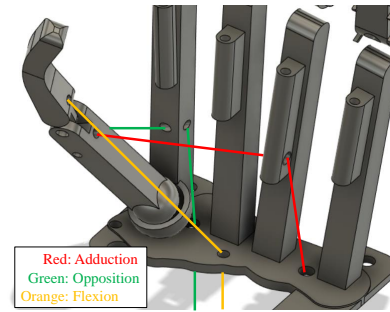


Fig. 8. Wire paths for thumb and metacarpal parts

B. How to Assemble the Robot Hand

This section describes the assembly method of the skin-skeleton integrated robot hand. This robot hand consists of only four parts (epidermal-skeletal integrated parts, metacarpal parts, basal and metacarpal bones of the thumb) and seven wires (Fig. 10). The epidermal parts are designed using the aforementioned method and consist of the skeleton excluding the metacarpals from the index finger to the little finger, plus the epidermis covering them. 3D printed parts are completed by washing and curing, and are designed to be more tear-resistant by curing for 60 minutes, which exceeds the recommended effect time of 25 minutes. In passing the wires through the holes inside the skeleton of those surface skin parts, problems occurred, such as the wires stopping inside the holes due to friction of the surface skin material, or the skeleton part breaking when pushed in. Therefore, we have prepared a wire bonded to a metal wire, and succeeded in simplifying the wire placement by threading the metal wire first. After penetration, the adhesive part of the wire and metal wire is cut off, and the ball-knotted piece is fixed with a UV-curable adhesive at the fingertip hole.

Parts other than the skin-skeleton integrated parts are fabricated by 3D printing with ABS filament. First, a thumb part with a wire and shaft attached is attached to the thumb part of the skin part. Then, seven wires from the thumb and four other fingers are threaded through the metacarpal part, placed inside the skin part, and fixed with screws to complete. The entire assembly time is less than one hour, indicating that it is extremely simple to assemble.

V. EXPERIMENTS

A. Items Grasping Task

Object grasping experiments were conducted to verify the basic performance of this robot hand. The classification of grasping forms based on Cutkosky's classification of human grasping behavior [18] is shown in Fig. 9. This classification is divided into Power Grasp, which uses finger bellies and palms and Precision Grasp, which uses the tips of fingers for grasping, and is further subdivided according to differences in grasp shape based on the shape of the object.

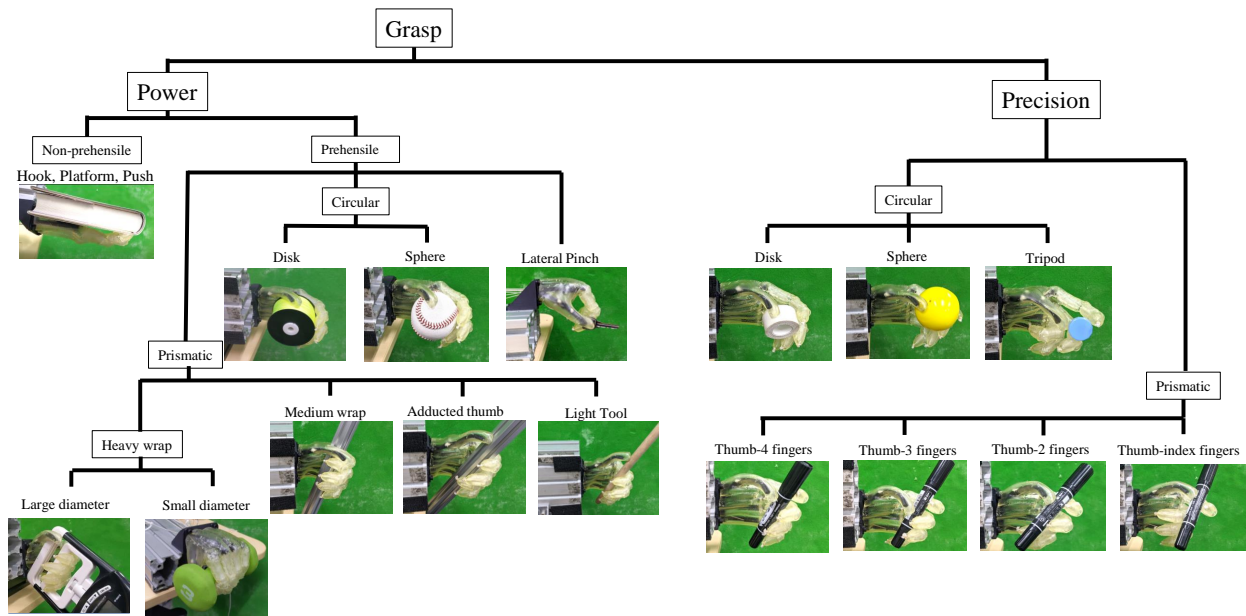


Fig. 9. Classification of grasping methods according to [18] and results of achieved grasps.

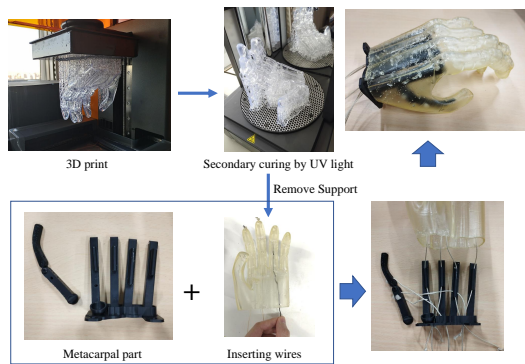


Fig. 10. Parts that compose a robot hand and assembly method

In this experiment, the muscle module [15] was connected to the seven tendons from the hand, and the muscle length was changed by an angular command while the object was fixed at a graspable point. The results of the grasping experiments are also shown in Fig. 9, and simple grasping of items such as Disk and Sphere was achieved with both the Power Grasp and Precision Grasp.

The detailed results of Power Grasp are described: Platform was achieved by placing a book on the palm of the hand without using actuators; Lateral Pinch was achieved by driving an actuator to hold the four fingers in a clenched position and to oppose the thumb. Adductive thumb was achieved by forcing the thumb into a fixed position and flexing the other four fingers, although this posture cannot be met by control due to the absence of an actuator for the thumb's return direction. The Light Tool was able to grasp a drumstick of 14[mm] in diameter, confirming that a highly accurate grip was achieved. With the Heavy Grasp, we used a grip strength tester and a dumbbell. The result of the grip strength meter was 1.4[kg], which was not sufficient. This

is thought to be because the subject was not able to clench his/her palm as well as humans do, and instead clenched the thumb and the other four fingers together. On the other hand, as for the dumbbell, it was able to grasp 3 pounds when the palm was placed parallel to the floor surface and 8 pounds when the palm was placed perpendicular to the floor surface, indicating that it has high grasping performance for small diameter objects.

Precision Grasp was able to grasp a wide variety of objects even at the fingertips because the finger bellies were deformable. In addition, each finger could be operated to realize four different grasping motions using the opposed thumb.

B. Dial Operation Experiment

In order to verify object manipulation by driving the thumb, an experiment to manipulate a dial was conducted. The experiment was started with the dial held between the thumb and the index finger, and the objective was to rotate the dial in a semi-clockwise direction by simultaneously performing adduction and opposition movements of the thumb and flexion movements of the index finger. In the experiment, the dial was rotated by pulling the tendon 9[mm] in thumb adduction, 9[mm] in thumb opposition, and 4[mm] in index finger flexion. The dials were from a power supply unit that was not connected to anything, and were tested to see if they varied from a display of 10[V] in the mode of varying voltage.

C. Impact Resistance Experiment

To verify the adaptability of the robot hand to the environment, a hammer impact was applied to the hand with and without tension. The direction of impact was palm, dorsal, and lateral. In all six types of experiments, the hammers passed through the impacts without any problem and returned

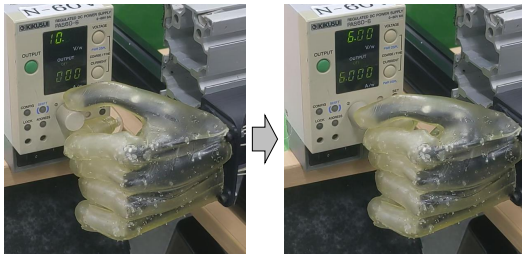


Fig. 11. Operation of dials with thumb and index finger

to their original positions within 1[s]. The results of the experiments are shown in Fig. 12.

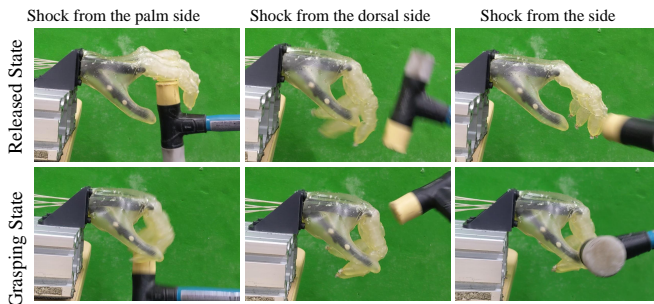


Fig. 12. Result of shock resistance experiment

VI. CONCLUSION

In this study, we proposed a skin-skeleton integrated robotic hand with the aim of fabricating a soft robotic hand that is both easy to assemble and complex to operate. While general robot hands have a problem that the number of parts increases with the number of degrees of freedom, this robot hand has 15 degrees of freedom and is composed of mostly single parts, which makes it easy to fabricate and assemble.

The most important element to realize a robot hand with multiple degrees of freedom with a single part is the skin-skeleton integrated part. This is a part that is a skin and skeleton formed at once from a flexible material, and it has no axes at all, yet it realizes 12 DOFs. To achieve this, the joints have a dorsal crease and a hole in the palm, which allow the joints to flex with little tension.

The thumb part is driven by three muscles, which are designed to be restored using the elasticity of the skin to obtain 3-DOFs by adding flexion to the 2-DOF joint structure. These three muscles were designed to realize a human grasping posture by referring to the muscle arrangement of the human body.

Grasping experiments were conducted to verify the performance of the fabricated skin-skeleton integrated robot hand. In the grasping experiment, all of the 16 grasping postures were achieved with human assistance, indicating the possibility of achieving movements similar to those of humans. In addition to grasping, dialing was also achieved,

indicating the possibility of extending tool manipulation by driving the thumb.

In this study, the thumb was driven by a simple muscle length command and was not controlled by the grasping state. In the future, we aim to obtain the status of each finger by placing sensors and performing other controls.

REFERENCES

- [1] K. Shimoga and A. Goldenberg, "Soft materials for robotic fingers," in *Proceedings 1992 IEEE International Conference on Robotics and Automation*, 1992, pp. 1300–1305 vol.2.
- [2] C. Firth, K. Dunn, M. H. Haeusler, and Y. Sun, "Anthropomorphic soft robotic end-effector for use with collaborative robots in the construction industry," *Automation in Construction*, vol. 138, p. 104218, 2022.
- [3] L. Tian, J. Zheng, N. Magnenat Thalmann, H. Li, Q. Wang, J. Tao, and Y. Cai, "Design of a single-material complex structure anthropomorphic robotic hand," *Micromachines*, vol. 12, no. 9, p. 1124, 2021.
- [4] A. A. Mohd Faudzi, J. Ooga, T. Goto, M. Takeichi, and K. Suzumori, "Index finger of a human-like robotic hand using thin soft muscles," *IEEE Robotics and Automation Letters*, vol. 3, no. 1, pp. 92–99, 2018.
- [5] A. Kochan, "Shadow delivers first hand," *Industrial Robot*, vol. 32, no. 1, pp. 15–16, 2005.
- [6] R. Deimel and O. Brock, "A novel type of compliant and underactuated robotic hand for dexterous grasping," *The International Journal of Robotics Research*, vol. 35, no. 1-3, pp. 161–185, 2016. [Online]. Available: <https://doi.org/10.1177/0278364915592961>
- [7] T. Hirose, S. Kitagawa, S. Hasegawa, Y. Kakiuchi, K. Okada, and M. Inaba, "Waterproof soft robot hand with variable stiffness wire-driven finger mechanism using low melting point alloy for contact pressure distribution and concentration," in *2022 IEEE 5th International Conference on Soft Robotics (RoboSoft)*, 2022, pp. 109–116.
- [8] P. Weiner, C. Neef, Y. Shibata, Y. Nakamura, and T. Asfour, "An embedded, multi-modal sensor system for scalable robotic and prosthetic hand fingers," *Sensors*, vol. 20, no. 1, p. 101, 2019.
- [9] H. Wang, F. J. Abu-Dakka, T. N. Le, V. Kyrki, and H. Xu, "A novel soft robotic hand design with human-inspired soft palm: Achieving a great diversity of grasps," *IEEE Robotics & Automation Magazine*, vol. 28, no. 2, pp. 37–49, 2021.
- [10] H. Wang, H. Xu, F. J. Abu-Dakka, V. Kyrki, C. Yang, X. Li, and S. Chen, "A bidirectional soft biomimetic hand driven by water hydraulic for dexterous underwater grasping," *IEEE Robotics and Automation Letters*, vol. 7, no. 2, pp. 2186–2193, 2022.
- [11] Y. She, C. Li, J. Cleary, and H.-J. Su, "Design and fabrication of a soft robotic hand with embedded actuators and sensors," *Journal of Mechanisms and Robotics*, vol. 7, no. 2, 2015.
- [12] C. De Pascali, G. A. Naselli, S. Palagi, R. B. Scharff, and B. Mazzolai, "3d-printed biomimetic artificial muscles using soft actuators that contract and elongate," *Science Robotics*, vol. 7, no. 68, p. eabn4155, 2022.
- [13] A. Mohammadi, J. Lavranos, H. Zhou, R. Mutlu, G. Alici, Y. Tan, P. Choong, and D. Oetomo, "A practical 3d-printed soft robotic prosthetic hand with multi-articulating capabilities," *PloS one*, vol. 15, no. 5, p. e0232766, 2020.
- [14] "Japanese hand measurements in anthropometric database national institute of aist 2012." [Online]. Available: 2.www.airc.aist.go.jp/dhrt/hand/index.htm
- [15] Y. Asano, T. Kozuki, S. Ookubo, K. Kawasaki, T. Shirai, K. Kimura, K. Okada, and M. Inaba, "A Sensor-driver Integrated Muscle Module with High-tension Measurability and Flexibility for Tendon-driven Robots," in *Proceedings of the 2015 IEEE/RSJ International Conference on Intelligent Robots and Systems*, 2015, pp. 5960–5965.
- [16] D. A. Neumann, *Kinesiology of the Musculoskeletal System: Foundations for Rehabilitation*. Mosby, 2013.
- [17] A. D. Nimbarte, R. Kaz, and Z.-M. Li, "Finger joint motion generated by individual extrinsic muscles: a cadaveric study," *Journal of orthopaedic surgery and research*, vol. 3, no. 1, pp. 1–7, 2008.
- [18] M. Cutkosky, "On grasp choice, grasp models, and the design of hands for manufacturing tasks," *IEEE Transactions on Robotics and Automation*, vol. 5, no. 3, pp. 269–279, 1989.